

# Pulse percolation conduction and multi-value memory

V. G. Karpov,<sup>1,\*</sup> G. Serpen,<sup>2,†</sup> Maria Patmiou,<sup>1,‡</sup> and Diana Shvydka<sup>3,§</sup>

<sup>1</sup>*Department of Physics and Astronomy, University of Toledo, Toledo, OH 43606, USA*

<sup>2</sup>*Department of Electrical Engineering and Computer Science, University of Toledo, Toledo, OH 43606, USA*

<sup>3</sup>*Department of Radiation Oncology, University of Toledo Health Science Campus, Toledo, OH 43614, USA*

(Dated: September 5, 2022)

We develop a theory of pulse conduction in percolation type of materials such as noncrystalline semiconductors and nano-metal compounds. For short voltage pulses, the corresponding electric currents are inversely proportional to the pulse length and exhibit significant nonohmicity due to strong local fields in resistive regions of the percolation bonds. These fields can trigger local switching events incrementally changing bond resistances in response to pulse trains. Our prediction opens a venue to a class of multi-value nonvolatile memory implementable with a variety of material systems.

## I. INTRODUCTION

Nonvolatile memory cells are often based on disordered materials, noncrystalline or compound, with percolation conduction. Percolation in these systems<sup>1–3</sup> is due to exponentially strong variations in local resistivities and the macroscopic conductivity is dominated by the clusters of the corresponding smallest random resistors allowing electric connectivity. Relevant for memory applications are percolation materials exhibiting plasticity, i. e. the ability to change their resistances in response to electric bias. They include metal oxides and chalcogenide compounds used respectively with resistive random access memory (RRAM)<sup>4</sup> and phase change memory (PCM),<sup>5</sup> granular metals,<sup>6</sup> and nano-composites.<sup>7</sup>

As a quick reminder, Fig. 1 shows random resistors forming bonds in a percolation cluster of correlation radius (mesh size)  $L_c$ . The standard treatment assumes time independent currents continuous through the bonds. Because the bond constituting microscopic resistors are exponentially different, the current continuity requires significantly different local electric fields through them. The highest of those local fields produces the exponentially strong nonohmicity of percolation materials.<sup>8–11</sup>

One distinct feature introduced here is that local electric fields in percolation bonds can be strong enough to structurally modify the underlying material through non-volatile changes in its local resistivities; hence, percolation with plasticity (PWP).

Another feature new to percolation analyses is the nonstationary pulse-shaped electric bias characteristic of nonvolatile memory operations. We will describe its related current-voltage characteristics and local switchings with fractional changes in the macroscopic resistance due to individual pulses. That feature appears similar to that of the spike-timing-dependent-plasticity (STDP) central to the functionality of neural networks (see<sup>12,13</sup> and references therein). From the practical standpoint, it paves a way to PWP multi-valued memory operated in the pulse regime and implementable with a variety of materials.

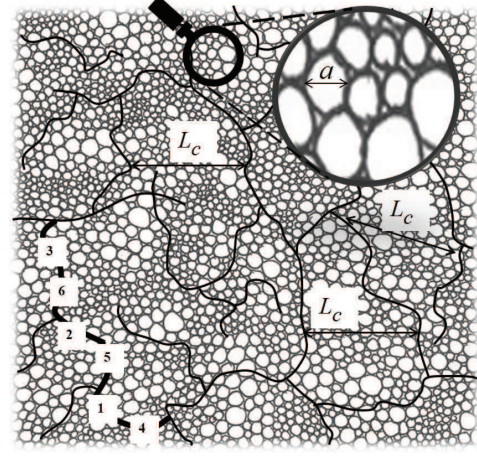


FIG. 1: A fragment of conductive pathways in the infinite percolation cluster representative of polycrystalline or granular materials. Numbers 1-6 represent random resistors in descending order of their resistances. The inset illustrates nonuniformity scale ( $a$ ), such as the diameter of nano-crystals.

## II. STANDARD PERCOLATION VS. PWP

We start our discussion by outlining the concept of standard percolation juxtaposed with that of PWP.

*Standard percolation*<sup>1–3</sup> is dominated by the sparse infinite conducting cluster between two large electrodes. That cluster's bonds consist of minimally strong resistors with total concentration sufficient to form a connected structure. It is effectively uniform over distances  $L \gg L_c$  (Fig. 1). Each bond consists of a large number ( $i = 1, 2, \dots$ ) of random resistors,  $R_i = R_0 \exp(\xi_i)$  where quantities  $\xi_i$  are more or less uniformly distributed in the interval  $(0, \xi_{\max})$ . The physical meaning of  $\xi$  depends on the type of system. For definiteness, we assume here  $\xi_i = V_i/kT$  corresponding to random barriers  $V_i$  in non-crystalline materials where  $k$  is the Boltzmann's constant and  $T$  is the temperature. In reality, the nature of percolation conduction can be more complex including e. g. finite size effects and thermally assisted tunneling between the microscopic resistors in nanocomposites.<sup>14,15</sup> These

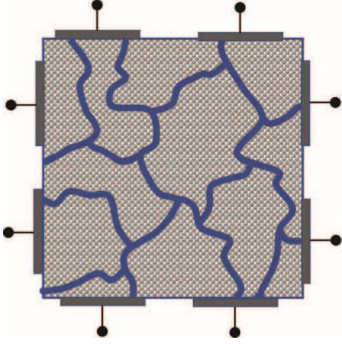


FIG. 2: Schematic 2D illustration of PWP with  $N = 8$  local interfaces (electrodes). Note a large combinatorial number  $N! = 8! \approx 4 \cdot 10^4$  of inter-electrode pathways.

complications will not qualitatively change our conclusions.

The microscopic resistors exhibit non-ohmicity<sup>9,11</sup> due to the field induced suppression of their original barriers  $V_i = kT\xi_i$ . A symmetric barrier of width  $a$  will be suppressed by  $qE_i a/2 = qU_i/2$ , where  $E_i$  and  $U_i$  are the field strength and voltage drop on  $i$ -th resistor, and  $q$  is the electron charge. As a result, the local current becomes,

$$I_i = I_0 \exp(-\xi_i) \sinh(qU_i/2kT) \quad (1)$$

where  $I_0$  is a constant.

Because of the continuity of electric current and resistors nonohmicity, the applied voltage concentrates on the strongest resistor of a percolation bond (resistor 1 in Fig. 1) suppressing it to the level of the next strongest (resistor 2 in Fig. 1), so the two equally dominate the entire bond voltage drop. It then suppresses the next-next strongest resistors, etc. As a result, the percolation cluster changes its structure, resulting in the macroscopic non-ohmic conductivity.<sup>8-11</sup>

Three assumptions underly the standard percolation theory: (a) The topology of infinite percolation cluster between two electrodes. (b) The volatility of bias induced changes: local resistances  $R_i$  adiabatically following voltages  $U_i$ . (c) The quasistatic nature of biasing steady over times exceeding the local relaxation times  $\tau_i$ , i. e.  $t \gg \tau_{\max} = \tau_0 \exp(\xi_{\max})$  where  $\tau_0 \sim 0.1 - 1$  ps depends on the type of system.

PWP systems violate all three of the above assumptions by: (a) opening a possibility of multiple ( $N \gg 1$ ) electrodes<sup>11</sup> as signal entrances/ports and not assuming the system dimensions exceeding  $L_c$  and requiring description beyond the standard percolation theory<sup>11,16</sup>; (b) allowing for bias induced nonvolatile changes; (c) operating under pulse shaped bias typical of neural networks (STDP). We address these differences as follows.

(a) Keeping in mind the case of multiple electrodes and/or below  $L_c$  system dimensions, we concentrate on the pulse non-ohmic conduction of a single percolation bond. The case of infinite cluster will be addressed in passing [see Eq. (8)]. (b) We will explicitly incorporate

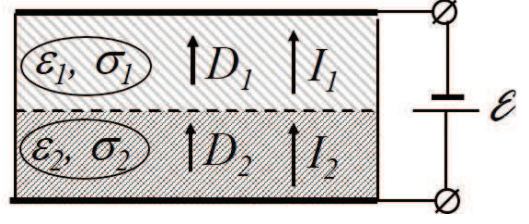


FIG. 3: A two layer system with dielectric permittivities  $\epsilon_1 \neq \epsilon_2$  and conductivities  $\sigma_1 \neq \sigma_2$ . The boundary conditions change from that of displacements,  $D_1 = D_2$ , for fast processes, to that of both  $D_1 = D_2$  and  $I_1 = I_2$  for slow processes implying an interface surface charge.

the possibility of nonvolatile changes. (c) We develop a theory of non-ohmic percolation in the pulse regime.

### III. NON-OHMIC PULSE PERCOLATION

Consider the non-ohmic conductivity of a series of random resistors,  $R_i = R_0 \exp(\xi_i)$  with  $\xi_i$  in  $(0, \xi_{\max})$  in response to a voltage pulse of length  $t$  [task (c) above]. A key addition to the standard dc analysis<sup>8</sup> is the separation of all resistors into two groups: ‘slow’ ( $\tau_i > t$ ) and ‘fast’ ( $\tau_i < t$ ). ‘Fast’ resistors maintain the current continuity adjusting their currents to local voltages  $U_i$  as described in Eq. (1). However, ‘slow’ resistors lag behind thus operating as capacitors. As a toy model, Fig. 3 presents a two-layer system with unequal dielectric permittivities and conductivities. The current through the layers becomes continuous ( $I_1 \equiv E_1 \sigma_1 = I_2 \equiv E_2 \sigma_2$ ) after a certain recharging time required to build a stationary interface charge layer; for fast processes, the field and current distributions are dominated by the continuity of electric displacements,  $D_1 \equiv E_1 \epsilon_1 = D_2 \equiv E_2 \epsilon_2$  while  $I_1 \neq I_2$ .

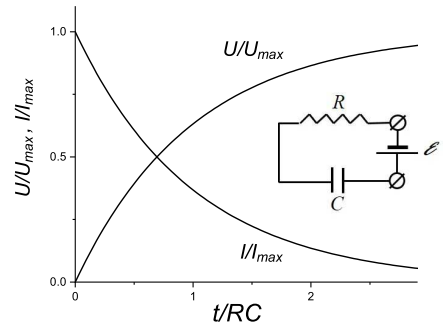


FIG. 4: A ‘textbook RC’ temporal dependencies for the circuit current and capacitor voltage ( $I_{\max} = \mathcal{E}/R$  and  $U_{\max} = \mathcal{E}$ ) where  $C$  represents the high resistance element of Fig. 3. A relatively small short-time voltage  $U$  corresponds to negligible voltage drops on ‘slow’ (large  $RC$ ) resistors.

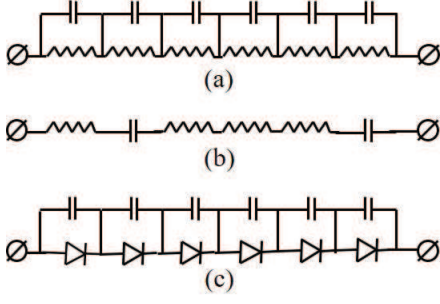


FIG. 5: Equivalent circuits relevant to pulse percolation conduction. (a) Each microscopic resistor has its related capacitance capable of bypassing the time dependent current. (b) The ‘fast’ resistors are represented as such, while ‘slow’ ones – as capacitors. (c) The nonlinear current-voltage characteristics of Eq. (1) are close to that of a diode; hence the circuit of diodes with capacitances allowing the numerical PSPICE modeling.

We assume  $\sigma_2 \gg \sigma_1$  to reflect the exponential dispersion of resistances in a percolation cluster, yet set  $\varepsilon_1 \sim \varepsilon_2$  corresponding to chemically-similar across layer materials. As a result, the short-time ratio of voltages across the layers is  $V_2/V_1 = \varepsilon_1/\varepsilon_2 \sim 1$ , while in the long-time regime, one gets  $V_2/V_1 = \sigma_1/\sigma_2 \gg 1$ , i. e. voltage drop in the high resistive layer is negligibly small.

The conductivities in the latter toy model can be related to the pulse duration through their corresponding Maxwell relaxation times  $t_{\sigma_{1,2}} = 1/(4\pi\sigma_{1,2})$ . The inequality  $\sigma_2 \gg t^{-1} \gg \sigma_1$  corresponds then to the case when the pulse is long enough to run significant current in layer 2, but not in layer 1. In terms of equivalent circuits, layer 2 will play the role of a resistor and layer 1 – that of a capacitor. The behavior of their series connection (Fig. 4) is consistent with the above conclusion of negligibly small voltage drop on ‘slow’ resistors.

Further equivalent circuit interpretation is illustrated in Fig. 5, which opens a pathway to PSPICE modeling. Some results of such modeling for a system (c) are presented in Fig. 6.

We conclude that the applied voltage is distributed mostly among the fast resistors. For that group, the voltage distribution is the same as for the dc voltage case,<sup>8</sup>

$$\sum_{\xi_i=\xi_0}^{\xi_t=\xi_t} U_i = V \quad \text{with} \quad \xi_t = \ln(t/\tau_0). \quad (2)$$

Here  $\xi_0$  corresponds to the smallest value resistor affected by the bias.

Presenting the total current in the form,

$$I = I_0 \exp(-\xi_0) \quad (3)$$

the condition of current continuity becomes,

$$\xi_0 - \xi_i = -qU_i/kT. \quad (4)$$

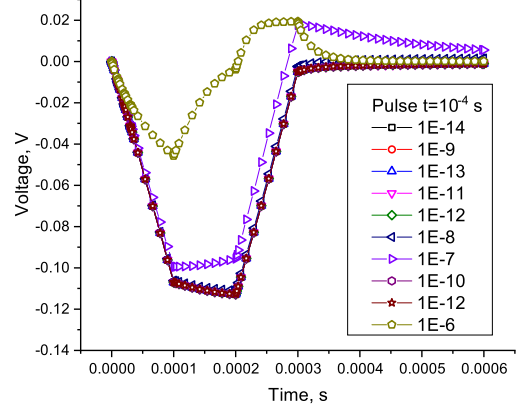


FIG. 6: PSPICE modeled pulses of voltage on each of a series of 10 diodes with exponentially different saturation currents (listed in Amperes). Each diode has a bypassing capacitor (of 1 nF) illustrated in Fig. 5(c). A 0.1 ms trapezoidal voltage pulse of amplitude 1 V was applied. The transient related shape features (charge/discharge) are irrelevant here. The results show how very low saturation current diodes are equally shunted by capacitors, while ‘fast’ diodes accommodate voltages logarithmic in their saturation currents – typical of dc regime.

Substituting the latter into Eq. (2) and replacing the sum with integral, yields,

$$\begin{aligned} \sum_{\xi_i=\xi_0}^{\xi_t=\xi_t} (\xi_0 - \xi_i) &= \int_{\xi_i=\xi_0}^{\xi_t=\xi_t} (\xi_0 - \xi) \frac{Nd\xi}{\xi_{\max}} \\ &= -\frac{N(\xi_t - \xi_0)^2}{2\xi_{\max}} = -\frac{qV}{kT} \end{aligned} \quad (5)$$

where  $N$  is the total number of resistors in the bond. The multiplier  $N/\xi_{\max}$  in the integrand of Eq. (5) is the probability density normalized to  $N$  resistors per bond. Note that  $\xi_{\max}/N_c \equiv \Delta\xi$  gives the average difference between two successive values of  $\xi$ ’s with  $N_c$  being the number of resistors per bond of the percolation cluster. Its numerical value is estimated as<sup>8,18</sup>  $\Delta\xi \sim 1$ .

Expressing

$$\xi_0 = \xi_t - \sqrt{(qV/kT)(2\xi_{\max}/N)} \quad (6)$$

and considering Eq. (3) yields,

$$I = I_0 \frac{\tau_0}{t} \exp \left( \sqrt{\frac{2\xi_{\max}}{N} \frac{qV}{kT}} \right). \quad (7)$$

This result applies when the pulse time  $t$  is shorter than the maximum relaxation time  $\tau_0 \exp(\xi_{\max})$  and is formally different from that of dc analysis<sup>8</sup> by the substitution  $\xi_{\max} \rightarrow \xi_t$  in Eq. (5). The two results coincide when  $\xi_t = \xi_{\max}$ . The dependence  $I \sim 1/t$  reflects the fact that the number of contributing ‘fast’ resistors decreases

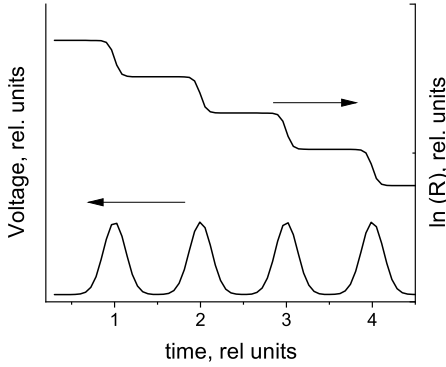


FIG. 7: Evolution of a PWP bond resistance  $R$  due to a train of pulses. Note the logarithmic scale for resistance changes.

along with  $t$ . We note that the scaling  $I \propto t^{-1}$  is close to the results of numerical modeling<sup>17</sup> for ac percolation current  $I \propto \omega$  when we set  $t \sim 1/\omega$ .

While we do not systematically consider the pulse conduction of the entire percolation cluster, it can be advanced based on the published approaches<sup>9,11</sup> with the above proposed modification,  $\xi_{\max} \rightarrow \xi_t = \ln(t/\tau_0)$ . This predicts the following current voltage characteristics,

$$I = I_0 \frac{\tau_0}{t} \exp \left( \sqrt{\frac{2a\mathcal{E}q}{3kT}} \ln \frac{t}{\tau_0} \right). \quad (8)$$

#### IV. PULSE INDUCED SWITCHING IN PWP

It follows from Eqs. (4) and (6) that the highest voltage drop is on the largest-valued resistor (1 in Fig. 1),

$$U_1 = V \sqrt{(kT/qV)(2\Delta\xi N_c/N)}, \quad (9)$$

which can be a significant fraction of the total applied voltage. The next high and other subsequent voltages (on resistors 2, 3, etc.) are incrementally smaller,  $U_{i+1} = U_i - \Delta\xi(kT/q)$ ,  $i = 1, 2, \dots$

Numerically, increment  $\Delta U = \Delta\xi(kT/q)$  can be quite appreciable,  $\Delta U \sim 0.05 - 0.1$  V corresponding to rather high operational temperatures  $T \sim 500 - 1000$  K of solid state memory cells.<sup>19</sup> Such  $\Delta U$  exceeds the observed statistical dispersion of threshold voltages<sup>20</sup> that is below 0.05 V. Therefore, local voltages  $U_i$  differ from each other enough to provide distinct switching events following the hierarchy of local resistors.

With the latter observation in mind, one can describe the pulse driven evolution of a PWP bond. Each microscopic bond element can exist in either high- or low-resistive state whose resistances,  $R_>$  and  $R_<$  are orders of magnitude different. Because of the inherent randomness, values of  $R_>$  form a broad spectrum, each well above  $R_<$ . Before pulse application, all the elements are in their high resistive state having random resistances

$R_>$ . The applied bias concentrated on the strongest resistor (in the manner of Fig. 1) will change it from  $R_>$  to  $R_<$  by switching, i. e. by long lived structural transformation not responsive to subsequent voltage variations. That process takes time  $t$  equal pulse length, since the highest affected resistor is defined by the condition that it accommodates voltage during that time. The end of the process coincides with the end of pulse, after which the system finds itself under no bias, with resistance decreased by a factor  $\eta \equiv \exp(\Delta\xi) \sim 3$ . The next pulse will similarly eliminate the second strong resistor decreasing the integral bond resistance by another factor  $\eta$ , etc. as illustrated in Fig. 7.

Note that the resistance graph in Fig. 7 presents the average picture: in reality, the spectrum of  $\xi_i$  is not equidistant leading to variations between the step changes in  $\ln R$ . Secondly, we have tacitly assumed instantaneous switching events. In reality, the switching time (between the field application and structural transformation) depends on the field strength and becomes sufficiently short (in sub-nanoseconds) for rather strong fields.<sup>20–25</sup> Here assumed strong fields  $U_i/a$  are realistic based on the typical values  $V \sim 10$  V,  $kT/q \sim 0.1$  V,  $\sqrt{(kT/qV)(2\Delta\xi N_c/N)} \sim 0.2$ , and  $a \sim 1$  nm, which yield  $U_1/a \sim 20$  MV/cm sufficient for switching.

#### V. MULTI-VALUE MEMORY

The sequences of stepwise resistance changes can be used as multiple memory records in PWP materials. The number of different memory values (steps) is estimated as  $M = (\xi_t - \xi_0)/\Delta\xi$ , i. e.,

$$M = \sqrt{(qV/kT)(2\xi_{\max}/N)}/\Delta\xi. \quad (10)$$

For a rough numerical estimate, we use as before  $qV/kT \sim 100$ , and  $2\xi_{\max}/N \sim \Delta\xi \sim 1$ , which yields  $M \sim 10$ . That number can be further increased by tweaking  $V$  and  $N$ . Combining the latter  $M \gg 1$  with large numbers of PWP pathways ( $N! \gg 1$  in Fig. 2) promises memory density above the current technology.

Two comments are in order here. First is that of the record erasing mechanisms. A possible answer refers to the known mechanisms of PCM and RRAM reset processes by Joule heat anneal and/or by using bipolar switching. For example, a moderate electric current during long enough time can anneal the pulse switched conducting regions to their original dielectric state. Alternatively, using materials with a degree of ferroelectricity can utilize the opposite polarity pulses for reverse switching.<sup>26</sup>

Secondly, our analysis of transport in a bond of random diodes might call upon building artificially assembled series of purposely different diodes. While they may be more controllable than the natural noncrystalline materials, their cost and dimensions remain questionable.

## VI. CONCLUSIONS

In conclusion, we have developed a theory of pulse non-ohmic transport in macro-bonds of percolation clusters. We have shown how voltage pulses can trigger subsequent

multiple switching events in microscopic regions of those macro-bonds incrementally changing the logarithms of their resistances. These changes pave a way to a class of superior multi-valued memory implementable with a variety of materials.

- 
- \* Electronic address: victor.karpov@utoledo.edu  
 † Electronic address: gursel.serpen@utoledo.edu  
 ‡ Electronic address: maria.patmiou@rockets.utoledo.edu  
 § Electronic address: diana.shvydka@utoledo.edu
- <sup>1</sup> B. I. Shklovskii, A. L. Efros, *Electronic Properties of Doped Semiconductors*, Springer, 1984.
  - <sup>2</sup> A. Y. Shik, *Electronic properties of inhomogeneous semiconductors*, Gordon and Breach (1995).
  - <sup>3</sup> A. A. Snarskii, I. V. Bezsudnov, V. A. Sevryukov, A. Morozovskiy, J. Malinsky, *Transport Processes in Macroscopically Disordered Media: From Mean Field Theory to Percolation*, Springer, New York (2016).
  - <sup>4</sup> M. Lanza, A Review on Resistive Switching in High-k Dielectrics: A Nanoscale Point of View Using Conductive Atomic Force Microscope, *Materials* **7**, 2155-2182 (2014); doi:10.3390/ma7032155
  - <sup>5</sup> A. Sebastian, M. Le Gallo and E. Eleftheriou, Computational phase-change memory: Beyond von Neumann computing, *J. Phys. D: Appl. Phys.* **52**, 44 (2019).
  - <sup>6</sup> I. A. Gladskikh, N. B. Leonov, S. G. Przhibelskii, and T. A. Vartanyan, The optical and electrical properties and resistance switching of granular films of silver on sapphire, *J. Opt. Technol.* **81** 280 (2014).
  - <sup>7</sup> Y. Song, H. Jeong, S. Chung, G. H. Ahn, T-Y Kim, J. Jang, D. Yoo, H. Jeong, A. Javey, T. Lee, Origin of multi-level switching and telegraphic noise in organic nanocomposite memory devices, *Scientific Reports*, **6**, 3967 (2016); DOI: 10.1038/srep33967.
  - <sup>8</sup> B. I. Shklovskii, Nonohmic hopping conduction, *Soviet Physics: Semiconductors*, **10**, 855 (1976) [*Fiz. Tekh. Poluprovodn.* **10**, 1440 (1976)]
  - <sup>9</sup> B. I. Shklovskii, Percolation mechanism of electrical conduction in strong electric fields, *Soviet Physics: Semiconductors*, **13**, 53 (1979) [*Fiz. Tekh. Poluprovodn.* **13**, 93 (1979)]
  - <sup>10</sup> D.I. Aladashvili, Z.A. Adamiya, K.G. Lavdovskii, E.I. Levin, and B.I. Shklovskii, Poole-Frenkel effect in the hopping conduction range of weakly compensated semiconductors, *Fiz. Tekh. Poluprovodn.* **23**, 213 (1989) [*Sov. Phys. Semicond.* **23**, 132 (1989)]
  - <sup>11</sup> Maria Patmiou, D. Niraula, and V. G. Karpov, The Poole-Frenkel laws and a pathway to multi-valued memory, *Appl. Phys. Lett.* **115**, 083507 (2019); https://doi.org/10.1063/1.5115991.
  - <sup>12</sup> I. R. Fiete, W. Senn, C. Z.H. Wang, and R.H.R. Hahnloser, Spike-Time-Dependent Plasticity and Heterosynaptic Competition Organize Networks to Produce Long Scale-Free Sequences of Neural Activity, *Neuron*, **65**, 563576 (2010).
  - <sup>13</sup> H. Markram, Wulfram Gerstner, P. J. Sjström, A history of spike-timing-dependent plasticity, *Frontiers in Synaptic Neuroscience*, **3**, Article 4 (2011); doi: 10.3389/fn-syn.2011.00004.
  - <sup>14</sup> K-C Lin, D. Lee, L. An, Y. H. Joo, Finite-Size Scaling Features of Electric Conductivity Percolation in Nanocomposites, *Nanoscience and Nanoengineering* **1**, 15 (2013); DOI: 10.13189/nn.2013.010103
  - <sup>15</sup> A. V. Eletskii, A. A. Knizhnik, B. V. Potapkin, J. M. Kenny, Electrical characteristics of carbon nanotube-doped composites, *Uspekhi Fizicheskikh Nauk* **185**, 225 (2015) [*Physics - Uspekhi* **58** 209 (2015)]; doi: https://doi.org/10.3367/UFNe.0185.201503a.0225
  - <sup>16</sup> M. E. Raikh and I. M. Ruzin, *Transmittancy fluctuations in randomly non-uniform barriers and incoherent mesoscopic in Mesoscopic Phenomena in Solids*, edited by B. L. Altshuller, P. A. Lee, and R. A. Webb, (Elsevier, New York, 1991), p. 315.
  - <sup>17</sup> T. B. Schroder and J. C. Dyre, ac Hopping Conduction at Extreme Disorder Takes Place on the Percolating Cluster, *Phys. Rev Lett.* **101**, 025901 (2008).
  - <sup>18</sup> E. I. Levin, I. M. Ruzin, B. I. Shklovskii, Transverse hopping conductivity of amorphous films in strong electric fields, *Soviet Physics: Semiconductors*, **22**, 401 (1987) [*Fiz. Tekh. Poluprovodn.* **22**, 642 (1987)]
  - <sup>19</sup> D. Niraula and V. G. Karpov, Heat Transfer in Filamentary RRAM Devices, *IEEE Transactions on Electron Devices*, **64**, 4106 (2017),
  - <sup>20</sup> I. V. Karpov, M. Mitra, D. Kau, G. Spadini, Y. A. Kryukov, and V. G. Karpov, Evidence of field induced nucleation in phase change memory, *Appl. Phys. Lett.*, **92**, 173501 (2008).
  - <sup>21</sup> V. G. Karpov, Y. A. Kryukov, I. V. Karpov and M. Mitra, Field-induced nucleation in phase change memory, *Phys. Rev. B*, **78**, 052201 (2008).
  - <sup>22</sup> D. Krebs, S. Raoux, C. T. Rettner, G. W. Burr, M. Salinga, M. Wuttig, Threshold field of phase change memory materials measured using phase change bridge devices. *Appl. Phys. Lett.* **95**, 082101, (2009); https://doi.org/10.1063/1.3210792.
  - <sup>23</sup> Y. Bernard, P. Gonon, and V. Jousseume, V. Resistance switching of Cu/SiO<sub>2</sub>Cu/SiO<sub>2</sub> memory cells studied under voltage and current driven modes. *Appl. Phys. Lett.* **96**, 193502, https://doi.org/10.1063/1.3428779 (2010).
  - <sup>24</sup> A. A. Sharma, I. V. Karpov, R. Kotlyar, J. Kwon, M. Skowronski, and J. A. Bain Dynamics of electroforming in binary metal oxide-based resistive switching memory. *J. Appl. Phys.* **118**, 114903, (2015); https://doi.org/10.1063/1.4930051.
  - <sup>25</sup> J. Yoo, J. Park, J. Song, S. Lim, H. Hwang, Field-induced nucleation in threshold switching characteristics of electrochemical metallization devices. *Appl. Phys. Lett.* **111**, 063109, (2017); https://doi.org/10.1063/1.4985165.
  - <sup>26</sup> V. G. Karpov, D. Niraula, I. V. Karpov, and R. Kotlyar, Thermodynamics of Phase Transitions and Bipolar Filamentary Switching in Resistive Random-Access Memory, *Phys. Rev. Applied*, **8**, 024028 (2017).